Model Parameter Identification of State of Charge Based on Three Battery Modelling using Kalman Filter

Lora Khaula Amifia, *Member, IAENG*

Abstract— **State of Charge (SOC) is the ratio of current versus total capacity of the battery. In the context of Battery Management System (BMS), the SOC is estimated by using a battery model. In this research, three battery models were presented, including (1) Thevenin battery model, (2) modified Thevenin battery model, and (3) simple battery model. Then, the SOC of those battery models was estimated using Coulomb Counting, Open Circuit Voltage (OCV), and Kalman Filter method. The simulation evaluated the performance of the SOC estimation methods, including the correctability of SOC initialization error. The simulation results showed that the proposed battery models could accurately estimate SOC. In terms of SOC initialization error, the Coulomb Counting, OCV Model 1, and OCV Model 2 could not correct the initialization error of SOC. However, the application of OCV Model 3 and Kalman Filter could provide an accurate SOC estimation with excellent correction of SOC initialization error. Compared to OCV model 3, the error correction in the Kalman Filter method was performed 25 minutes faster. Therefore, this finding suggests that Kalman Filter is the most suitable estimation method for BMS due to the high accuracy of SOC estimation (RMSE = 0.0014) and fast correction of SOC initialization error (time < 20 seconds).**

Index Terms—**State of Charge, Battery Management System, Battery Modelling, Kalman Filter, Coulomb Counting, Open Circuit Voltage.**

I. INTRODUCTION

TECHNOLOGY in transportation is rapidly developed in several countries. The ultimate goal of the transportation technology development is to reduce the usage of fossil fuels, i.e., gas and diesel in vehicle since it contributes to the increase of global warming [1]. By 2050, it is predicted that electric vehicles (EV) can potentially reduce CO_2 up to 21%. Thus, research about the electrical vehicle is important to be done. One of the pivotal component in electric vehicle development is the battery, which is the energy storage that enable the whole operations of an electric vehicle [2],[3].

A battery is an instrument to collect and generate electricity that can act as energy storage and source. Nowadays, batteries are widely applied from simple devices, such as mobile phones and portable computers, to essential and robust devices, such as the Uninterruptible Power Supply (UPS) [4]. Due to the shift from internal combustion engine to the electrical engine, the automotive world has started to use batteries as in hybrid EVs or even fully EV [5].

As the battery has been used over time, the galvanic cells in the battery experience degradation, leading to the reduction of battery capacity. Proper battery conditioning can reduce the occurrence of such degradation in a battery [6]. This conditioning process, which may include battery state monitoring, battery protection, or battery balancing, can be done using a battery management system (BMS) - a system to manage the battery not merely limited to electronics systems and mechanical systems [7]. By doing the battery conditioning, the BMS can ensure the optimum energy usage of the battery and keep the battery from failure risk, thus preserving the battery capacity of an EV.

The BMS includes the algorithm of battery state estimation. The battery modelling, in this case, plays a vital role in the algorithm used in the BMS to predict the voltage response of the battery [8],[9]. Several studies have been done related to battery modellings, such as mathematical models, electrochemical models, and equivalent circuit models (ECM) [10].

Mathematical models can be analytical or stochastic [11],[12]. Meanwhile, battery properties are explained as several formula combinations of different physical concepts in analytical models. For the stochastic one, the probability of the battery properties is forecasted based on the current state of the battery. In electrochemical models, the battery is modelled using the battery's chemical properties in which this model can provide complete information in an exchange of complex calculations [13],[14]. In ECM, the battery is modelled as a combination of electronic components such as a resistor, capacitor, and voltage source. Compared to mathematical and electrochemical models, the ECM explains the battery properties with the necessary of accuracy and simplicity [15]. Therefore, the ECM is more suitable to be used in microprocessors and real-time applications such as the EV.

There are several ECM-based models, such as the Thevenin-battery model and the Rint battery model. The Thevenin battery model consists of a parallel RC circuit with one ladder or several ladders. The complex differential equation of the parallel RC circuit is transformed into a discrete form to simplify the analysis of the battery

Manuscript received September 13, 2021; revised July 6, 2022. This work was supported in part by Institut Teknologi Telkom Surabaya grant.

Lora Khaula Amifia is a Lecturer at the Faculty of Electrical Technology and Intelligent Industry, Institut Teknologi Telkom Surabaya, Surabaya, Indonesia, corresponding author email: loraamifia@ittelkom-sby.ac.id; Phone: +6282143903133.

parameter [16]. Then, the RLS method is used to obtain the battery parameters by giving current and voltage to the battery [17]. The Thevenin model is more accurate than the Rint battery model, with only one resistor for system load calculation [18],[9]. Hence, many researchers prefer to use this model to estimate the battery parameter and monitor the change of a parameter.

The effect of different battery state estimation methods on each model has not been investigated yet. The battery state estimation in BMS may include the State of Charge (SOC), State of Health (SOH), Fault Detection, Cell Balancing, and Current Sensorless [19]. The first thing to be noticed in preserving the battery capacity is the SOC which is the most important part in the battery problem [20],[21]. This paper will focus the discussion on the SOC estimation as a representation of the battery capacity. SOC is a ratio between the remaining charge and the battery's total charge, which commonly expressed in percentages from 0% to 100%. The SOC cannot be measured directly by using a sensor; hence, an algorithm is needed to estimate it.

SOC estimation can be divided into soft computing and hard computing categories. Soft computing such as neural networks and fuzzy inference systems may estimate the battery's state accurately with the addition of tuning ability [22]. However, it is difficult to implement the soft computing method to a dynamic battery system model [23]. Large computations might be required to tune the estimation parameter, i.e., neural network weight and fuzzy membership functions. In this case, hard computing methods, such as Coulomb Counting, Open Circuit Voltage (OCV), and Kalman Filter, are preferable rather than the soft one for simplifying the computation process [24].

The Coulomb Counting method can be used to estimate the SOC as an integration of current over time [25],[26]. However, it also has some weaknesses: high accuracy is needed, and there is a high possibility of error accumulation during estimation. Meanwhile, the OCV method calculates the steady voltage of an open circuit in the model related to charging and discharging history [27]. This method can estimate the SOC accurately, but the battery takes long adequate resting before estimation. Besides, the OCV can only be used in an open circuit situation, which is unlikely to occur during EV operation [28],[29].

Other SOC estimation research based on ECM have been conducted using Kalman Filter, which estimates a system measurement using the system's state. It has been used to solve problems of filtering discrete data such as the battery model [21]. There are several variations of KF such as extended KF (EKF), Adaptive Extended KF (AEKF), and Square Root Unscented KF using Spherical Transform (Sqrt-UKFST). The KF method does not require any circuit to be an open circuit; thus, it can be implemented in EV [30]. Moreover, it can correct the SOC initialization error that occurs during the operation of an EV. The more advanced the KF is, the more accurate the SOC estimation. However, the amount of computation may increase [31].

The combination of battery models and estimation method determines the estimation accuracy. Therefore, this research compared the estimation performance based on a combination of battery models and SOC estimation methods. Three battery models were used, including (1) Thevenin battery model, (2) modified Thevenin battery model, and (3) Rint simple battery model. Then, simulations of the SOC estimation methods mentioned above were conducted on each model. Pulse test and Dynamic Stress Test (DST) were also used for further analysis. Then, the accuracy for each SOC estimation method was determined by calculating the error percentage, mean-square error (MSE), and root means square error (RMSE).

II. Battery Modelling

Identification of battery parameters requires appropriate battery modelling. Battery modelling is important before simulating an Electric Vehicle and developing the Battery Management System [6]. It is necessary to apply the SOC estimation algorithm accurately to produce an optimal function of the BMS [32]. Battery modelling in this paper was carried out using Thevenin equivalent circuit model (model 1), Thevenin modification (model 2), and simple battery modelling (model 3), considering their complexities, modelling accuracies, and reliabilities while representing the dynamic properties of the battery.

A. Thevenin Model (Model 1)

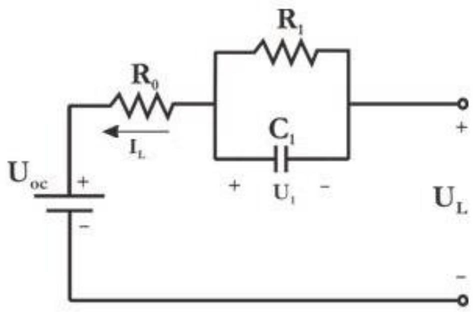

Fig. 1. Thevenin Battery Model (Model 1)

As an analytical tool, Thevenin model a complex circuit into a simple one by making a circuit replacement in the form of a voltage source made in series with an equivalent resistance. Thus, it is excellent to be applied to analyze battery circuit systems. The most commonly used Thevenin battery model uses a parallel *RC* circuit, as shown in Figure 1. In Figure 1, U_L is the terminal voltage, U_{oc} is the open-circuit voltage, R_0 is the internal resistance, C_1 is the polarization capacitance, and R_1 is the polarization resistance. They represent the transient response characteristics during the charging and discharging process. U_1 is the voltage on C_1. Based on the Thevenin model as shown in Figure. 1, some equations can be derived.

$$U_L(s) - U_{OC}(s) = I_L(s)\left(R_o + \frac{R_1}{1 + R_1C_1s}\right) \tag{1}$$

where E_L=U_L-U_{OC}. Then, the transfer function *G(s)* based on (1) can be written as follows,

$$G(s)=\frac{E_L(s)}{I_L(s)}=+R_0+\frac{R_1}{1+R_1C_1s}=\frac{R_0+R_1+R_0R_1C_1s}{1+R_1C_1s} \tag{2}$$

Equation (2) is discretized using Bilinear Transformation as in (3)

$$s=\frac{2}{T}\frac{1-z^{-1}}{1+z^{-1}} \tag{3}$$

where z is a discrete operator so that the following equation can be obtained

$$G(z^{-1})=\frac{\frac{R_0T+R_1T+2R_0R_1C_1}{T+2R_1C_1}+\frac{R_0T+R_1T-2R_0R_1C_1}{T+2R_1C_1}z^{-1}}{1+\frac{T-2R_1C_1}{T+2R_1C_1}z^{-1}} \tag{4}$$

Based on (4), some variables can be assumed as follows,

$$a_1=-\frac{T-2R_1C_1}{T+2R_1C_1}, \tag{5}$$

$$a_2=\frac{R_0T+R_1T+2R_0R_1C_1}{T+2R_1C_1}, \tag{6}$$

$$a_3=\frac{R_0T+R_1T-2R_0R_1C_1}{T+2R_1C_1} \tag{7}$$

Therefore, the values of the Thevenin model parameters can be calculated using the following equations

$$R_0=\frac{(a_2-a_3)}{1+a_1}; \tag{8}$$

$$R1=\frac{2(a_1a_2+a_3)}{1-a_1^2}; \tag{9}$$

$$C_1=\frac{T(1+a_1)^2}{4(a_1a_2+a_3)} \tag{10}$$

After discretization, Equation (1) can be written as in the equation below, where $k=1,2,3,\ldots$.

$$E_L(k)=a_1E_L(k-1)+a_2I_L(k)+a_3I_L(k-1) \tag{11}$$

The potential difference of the open-circuit is affected by a function of time *(t)*, which can be defined as the open-circuit voltage function. It can be described as a function of *SOC*, *Tem*, and *H* as written in the following Equation,

$$U_{OC}=f(SOC(t),Tem(t),H(t)) \tag{12}$$

Then, the U_{OC} in Equation (12) is derived into the equation below

$$\frac{dU_{OC}}{dt}=\frac{\partial U_{OC}}{\partial SOC}\frac{\partial SOC}{\partial t}+\frac{\partial U_{OC}}{\partial Tem}\frac{\partial Tem}{\partial t}+\frac{\partial U_{OC}}{\partial H}\frac{\partial H}{\partial t} \tag{13}$$

Equation (13) can be simplified to (14) after considering several assumptions: $dSOC/dt\approx 0$ for low-energy batteries; the cooling/heating that BMS is experiencing is insignificant for normal operation $dTem/dt\approx 0$, and $dH/dt\approx 0$ for the battery is assumed to be new.

$$\frac{dU_{OC}}{dt}=\frac{U_{OC}(k)-U_{OC}(k-1)}{T}\approx 0 \tag{14}$$

$$\Delta U_{OC}(k)=U_{OC}(k)-U_{OC}(k-1)\approx 0 \tag{15}$$

Then, Equation (11) can be written as,

$$U_L(k)=(1-a_1)U_{OC}(k)+a_1U_L(k-1)+a_2I_L(k)+a_3I_L(k-1) \tag{16}$$

with,

$$\varphi_1(k)=[1\quad U_L(k-1)\quad I_L(k)\quad I_L(k-1)], \tag{17}$$

$$\theta_1(k)=[(1-a_1)U_{OC}(k)\quad a_1\quad a_2\quad a_3]^T \tag{18}$$

$$y_k=U_L(k)$$

$$y_k=\varphi_1(k)\theta_1(k) \tag{19}$$

The values of $U_L(k)$ and $I_L(k)$ were sampled using a constant period for an online application. Meanwhile, vector θ_1 was identified using the RLS (Recursive Least Square) algorithm according to (19), and the model parameters can be found using (9).

According to Thevenin's model shown in Figure. 1, the open-circuit voltage can also be written as

$$U_{OC}=U_L+U_{R0}+U_1 \tag{20}$$

The current on the parallel *RC* circuit can be written as follows,

$$I_L=C_1\frac{dU_1}{dt}+\frac{U_1}{R_1} \tag{21}$$

Therefore, the first derivation of voltage at the capacitance (U_1) can be expressed by

$$\dot{U}_1=\frac{I_L}{C_1}-\frac{U_1}{R_1C_1} \tag{22}$$

According to the Coulomb Counting method, the *SOC* equation is expressed as follows,

$$SOC=SOC_0+\frac{1}{C_N}\int_{t_0}^{t}I\cdot d\tau \tag{23}$$

and its first derivation is expressed by

$$s\dot{o}c=\frac{1}{C_N}I \tag{24}$$

The voltage at the capacitance and the *SOC* are taken as the states of the battery. Referring to (22) and (24), the state-space model can be mathematically written as the following equation.

$$\begin{bmatrix}\dot{U}_1\\ s\dot{o}c\end{bmatrix}=\begin{bmatrix}-\frac{1}{R_1C_1} & 0\\ 0 & 0\end{bmatrix}\begin{bmatrix}U_1\\ soc\end{bmatrix}+\begin{bmatrix}\frac{1}{C_1}\\ \frac{1}{C_N}\end{bmatrix}I_L \tag{25}$$

Thus, the battery model needs two input parameters.

B. Modified Thevenin Model (Model 2)

Similar to the previous modelling, Model 2 used the Thevenin battery model. However, a capacitance load is used in this model rather than a voltage source. If U_{OC} was used in the first model, model 2 modified it as U_C. Therefore, some parameters used in this model are C, R_0, R_1, and C_1, as shown in Figure 2.

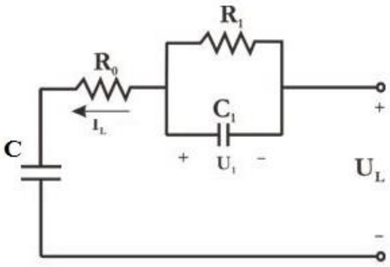

Fig. 2. Thevenin Modified Battery Model (Model 2)

Based on Model 2, the voltage at the capacitance C can be expressed as the following equation.

$$U_C = \frac{1}{C}\int I_L\,dt \tag{26}$$

Since $U_C = U_{OC}$ the first differential equation of (26) can be expressed as

$$\dot{U}_{OC} = \frac{1}{C} I_L \tag{27}$$

Due to the similarity, the voltage at capacitance C_1 and its first derivation are the same as the previous model. Thus, the state-space model for Model 2 can be established by rewriting equations (24) and (27) as in the equation below.

$$\begin{bmatrix} \dot{U}_1 \\ \dot{U}_{OC} \end{bmatrix} = \begin{bmatrix} -\frac{1}{R_1C_1} & 0 \\ 0 & 0 \end{bmatrix} \begin{bmatrix} U_1 \\ U_{OC} \end{bmatrix} + \begin{bmatrix} \frac{1}{C_1} \\ \frac{1}{C} \end{bmatrix} I_L \tag{28}$$

C. Rint Model (Model 3)

The Rint mathematical circuit model is shown in Figure 3, consisting of resistance R, capacitance C, capacitance-voltage V_C, and the voltage barriers V_R. The relationship of terminal voltage V_t with the voltage on the capacitor V_C; terminal voltage V_t with the voltage barriers V_R, can be represented by Laplace equations below.

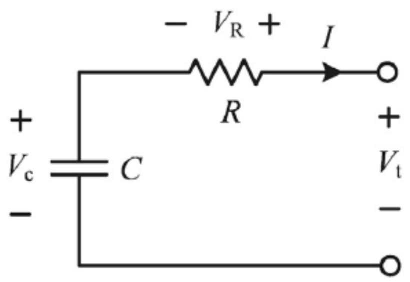

Fig. 3. Simple Model (Model 3)

$$\frac{V_C}{V_t} = \frac{1}{1 + sRC} \tag{29}$$

$$\frac{V_R}{V_t} = \frac{sRC}{1 + sRC} \tag{30}$$

Next, Equation (29) is returned to the time domain. Equation (31) is the differential equation of V_C, which requires sampling time Ts.

$$\frac{dV_C}{dt} \approx \frac{V_C[k] - V_C[k-1]}{T_s} \tag{31}$$

Therefore, Equation (29) can be rewritten into (32), and its coefficient was simplified using the formulation in Equation (33).

$$V_C[k] = V_C[k-1]\cdot(1-\alpha) + V_t[k]\cdot\alpha \tag{32}$$

$$\alpha = \frac{T_s}{T_s + RC} \tag{33}$$

Based on the relationship between voltage and current at the resistance (Ohm's Law), then Equation (30) can be transformed into (34).

$$\frac{I}{V_t} = -\frac{sC}{1 + sRC} \tag{34}$$

If the same method for estimating the capacitance-voltage is applied to Equation (34), then the estimated current equation can be obtained as follows,

$$I[k] = (1-\alpha)\cdot\left(I[k-1] + \frac{V_t[k] - V_t[k-1]}{R}\right) \tag{35}$$

III. State of Charge Estimation

One of the battery modelling applications in BMS is SOC estimation. SOC represents battery capacity and cannot be measured directly using a sensor. One method for measuring SOC is to use Coulomb Counting, i.e., the integration of current over time [33]. Meanwhile, Kalman Filter is a method to estimate a problem using the system states and make a minimum variance in the search process for optimal estimates in a system and a solution used to solve linear discrete data filtering problems [14]. The method is profoundly suitable for SOC estimation to obtain an effective and efficient BMS. Another estimation method, i.e., Open Circuit Voltage (*OCV*), can also be used.

A. State of Charge (SOC)

According to Equation (11), the estimated *OCV* and current can be obtained. Meanwhile, according to Equation (15) and the differential form equation of *SOC* in Equation (37), the relationship between capacitance C, battery capacity Cn, and the *OCV-SOC* relationship can be expressed as Equation (38), because the capacitance-voltage can be considered as OCV. Thus, the capacitor in the *RC* battery model shown in Figure 3 can be written as follows,

$$I = -C\frac{dV_c}{dt} \tag{36}$$

$$\frac{dSOC}{dt} = -\frac{I}{C_n} \tag{37}$$

$$C = C_n\frac{dSOC}{dOCV} \tag{38}$$

The initial *SOC* is critically important. It can be obtained from the *OCV-SOC* relationship, by providing the initial terminal voltage as the initial *OCV* from the *SOC* information and Equation (37). Then, the battery *SOC* can be calculated using the Coulomb Counting method.

The coulomb Counting is the most widely used method to estimate *SOC*. It can measure the battery capacity by observing the changes of the remaining charge based on electrical current into or outro the battery cells [34]. This method can be formulated into:

$$SOC = SOC_0 - \frac{1}{C_{cap}}\int_0^t \eta\, I_{batt}\, dt, \tag{39}$$

$$\dot{SOC} = -\frac{\eta\, I_{batt}}{C_{cap}} \tag{40}$$

where Columbic coefficient η is a constant value of 1 during discharging and 0.98 in charging. SOC_0 is the initial value of SOC that indicates the value of SOC shortly before I_{batt} flows into or out of the battery cells. C_{cap} capacity indicates the maximum capacity of new battery cells.

B. Kalman Filter

Kalman Filter is one method to estimate a problem using the system's state; the core of this theory is how to make the minimum variance in finding the optimal estimates on a system [35]. It is a recursive process that is effective when dealing with measurement data that have noises; either by combining it with other sensor measurement data or by filtering the noise itself [36].

Kalman Filter acts as a solution for data-screening discrete linear recursive process, which Rudolf E. Kalman first introduced in 1960. Also, Kalman Filter assumed all estimated states linear, and all observed variables can be represented in Gaussian distribution [37]. It supports the estimation of states based on their previous and current records, and it can be performed even when the estimated model system's nature is unknown.

Kalman Filter model assumes the estimation based on the following equations.

$$x_{k+1} = Ax_k + Bu_k + w_k \tag{41}$$

with the measurement process $z \in \Re^m$:

$$z_k = Cx_k + v_k \tag{42}$$

where,

x_k = process state at time *k*
A = transition matrix
u_k = input control at time *k*
B = constant matrix for u_k
w_k = process noise
z_k = variable measurement results at time *k*
C = measurement matrix
v_k = measurement noise

Then, the error covariance matrix can be calculated as:

$$P_{k|k-1} = AP_{k-1|k-1}A^{\mathrm{T}} + Q_k \tag{43}$$

While the Kalman Gain can be defined as follows.

$$K_k = P_{k|k-1}C^T\left(CP_{k|k-1}C^T + R\right)^{-1} = \frac{P_{k|k-1}C^T}{CP_{k|k-1}C^T + R} \tag{44}$$

Each estimated state will be updated based on the following equation.

$$x_{k|k} = x_{k|k-1} + K_k(z_k - Cx_{k|k-1}) \tag{45}$$

After the state is updated, the error covariance matrix is also updated according to the equation below.

$$P_{k|k} = (I - K_kC)\, P_{k|k-1} \tag{46}$$

C. SOC Estimation using Coulomb Counting Method

SOC estimation using Coulomb Counting is done by integrating current over time. In the research, the application of this method was tested using two loading data: pulse current load and variable current.

$$SOC = SOC_0 + \frac{1}{C_N}\int_{t_0}^{t} I \cdot d\tau \tag{47}$$

If Equation (47) is converted into an equation in discrete form, the equation will become:

$$SOC_k = SOC_{k-1} + \frac{1}{C_N} I_k .\, d\tau \tag{48}$$

D. SOC Estimation using OCV Method

SOC estimation using the OCV method can be done using a lookup table or obtained from the OCV function. The SOC value as a function of OCV is obtained as in Equation (49). It is chosen as a 10-orde polynomial function because it provided the smallest Root Mean Square Error (RMSE) based on testing results for orders 5 to 11 in Table I.

TABLE I
POLYNOMIAL OCV-SOC ERRORS

Order	RMSE
5	0.004631
6	0.003227
7	0.003205
8	0.003205

9	0.003189
10	0.003188
11	0.003189

$$SOC(x) = k_1x^{10} + k_2x^9 + k_3x^8 + k_4x^7 + k_5x^6 + k_6x^5 + k_7x^4 + k_8x^3 + k_9x^2 + k_{10}x + k_{11} \tag{49}$$

where x = OCV,

The values of the constants are presented as follows.

k_1=	0.122471377846543	k_7=	-17.9445309835419
k_2=	-1.72484699277323	k_8=	3981.29280161986
k_3=	5.96819898553211	k_9=	7837.19843244986
k_4=	11.4868086091382	k_{10}=	-72674.9683228613
k_5=	-43.3488086640324	k_{11}=	97461.8813096120
k_6=	-254.299496750849		

In Model 1, the estimated value of *OCV* was obtained from the parameter identification process. The identification process was carried out using the Recursive Least Square method, with one of the estimated weights being the *OCV* value.

Whereas in Model 2, the *OCV* (U_{OC}) value was the state value in the state-space model such as the following.

$$\begin{bmatrix} \dot{U_1} \\ \dot{U_{OC}} \end{bmatrix} = \begin{bmatrix} \frac{1}{R_1C_1} & 0 \\ 0 & 0 \end{bmatrix} \begin{bmatrix} U_1 \\ U_{OC} \end{bmatrix} + \begin{bmatrix} \frac{1}{C_1} \\ \frac{1}{C} \end{bmatrix} I_L \tag{50}$$

While in Model 3, the *OCV* value was obtained using the recursive Equation (32). After the three *OCV* estimates were obtained, the *OCV* value was entered into the *OCV* function to get the *SOC* value.

E. SOC Estimation using Kalman Filter Method

The SOC estimation using Kalman Filter was applied to two different battery models. In Model 1, the states used were U_1 and *SOC*. While in Model 2, the states used were U_1 and U_{OC}. The function of *SOC* used for estimation using Kalman Filter is expressed in the equation below.

$$SOC(x) = a_1x^{10} + a_2x^9 + a_3x^8 + a_4x^7 + a_5x^6 + a_6x^5 + a_7x^4 + a_8x^3 + a_9x^2 + a_{10}x + a_{11} \tag{51}$$

1) Model 1

The Kalman Filter model considers noise, so the state-space model in Equation (28) needs to be added with W_k noise modelling. It also needs to be discretized using backward Euler. The final model of Kalman Filter used for Model 1 is shown in Equation (52)

$$\begin{bmatrix} \dot{U_1}_k \\ soc_k \end{bmatrix} = \begin{bmatrix} \frac{1}{R_1C_1} & 0 \\ 0 & 0 \end{bmatrix} \begin{bmatrix} U_{1\,k-1} \\ soc_{k-1} \end{bmatrix} + \begin{bmatrix} \frac{1}{C_1} \\ \frac{1}{C_N} \end{bmatrix} I_{L\,k-1} + W_k \tag{52}$$

where W_k is the process noise.

The measurement output is defined by

$$z_k = OCV(SOC) + I_LR_0 + U_1 + V_k \tag{53}$$

where the *OCV(SOC)* is the *OCV* value obtained from the *SOC* function with the 10th-order polynomial equation above.

Some initializations need to be made for x_0, P_0, Q_0, and R. The initialization value of $R = 10$. The R-value is the initial measurement noise covariance value. It was obtained by considering the accuracy of the sensor and the estimation results. It was chosen based on measurement fluctuations that are far from the actual average obtained by measuring the noise variance on the sensor. Furthermore, the value of R was determined through experiments which resulted in a good accuracy of SOC estimation.

Meanwhile, Equation (54) is the initial state value of the state-space model. The initial value for the first state was zero, while the second state, which is *SOC*, was initialized according to the actual *SOC* value.

$$x_0 = \begin{bmatrix} 0 \\ SOC_{inisial} \end{bmatrix} \tag{54}$$

Equation (55) is the initial error covariance value. The small value indicates confidence in the small estimation error so that the effort made for error correction is small. In addition, a small error covariance value is also intended to observe changes in the estimated value to the actual value.

$$P_0 = \begin{bmatrix} 0{,}1 & 0 \\ 0 & 0{,}1 \end{bmatrix} \tag{55}$$

Equation (56) below is the initial value of the process error variance.

$$Q_0 = \begin{bmatrix} 0{,}1 & 0 \\ 0 & 0{,}1 \end{bmatrix} \tag{56}$$

The initialization value was made small because process noise could not be calculated. However, model predictions were assumed to be good because model validation resulted in a small error.

2) Model 2

Similarly, the state-space model in Equation (28) needs to be added with noise and be discretized. The resulting Kalman Filter model for Model 2 is expressed as

$$\begin{bmatrix} \dot{U_1}_k \\ soc_k \end{bmatrix} = \begin{bmatrix} \frac{1}{R_1C_1} & 0 \\ 0 & 0 \end{bmatrix} \begin{bmatrix} U_{1\,k-1} \\ soc_{k-1} \end{bmatrix} + \begin{bmatrix} \frac{1}{C_1} \\ \frac{1}{C_N} \end{bmatrix} I_{L\,k-1} + W_k \tag{57}$$

The measurement output is defined by

$$z_k = U_{OC} + I_LR_0 + U_1 + V_k \tag{58}$$

The initialization for x_0, P_0, Q_0, dan R is as follows,

$$x_0 = \begin{bmatrix} 0 \\ U_{OC\ inisial} \end{bmatrix} \tag{59}$$

$$P_0 = \begin{bmatrix} 0{,}1 & 0 \\ 0 & 0{,}1 \end{bmatrix} \quad (60)$$

$$Q_0 = \begin{bmatrix} 0{,}1 & 0 \\ 0 & 0{,}1 \end{bmatrix} \quad (61)$$

with the value of $R = 10$.

IV. Result and Analysis

A. SOC Estimation Results with Pulse Test Data

The comparison of SOC estimation results from different methods will be discussed in the section. Generally, the SOC estimation results looked similar for each, as seen in Figure 4. However, the SOC final value obtained was found different by using similar test data, i.e., the pulse test.

TABLE II
Error in SOC Estimation with Pulse Test Data

Method	Final SOC	% ERROR	MSE	RMSE
CC	1.44%	1.667	8.3×10^{-5}	0.0101
OCV 1	1.32 %	1.49	6.6×10^{-5}	0.0081
OCV 2	-0.11 %	1.013	2.9×10^{-5}	0.0054
OCV 3	1.23 %	2.36	14.5×10^{-5}	0.0121
KF 1	0.00 %	0.76	1.4×10^{-5}	0.0038
KF 2	0.00 %	0.92	2.05×10^{-5}	0.0045

[a]CC = Coulomb Counting, OCV = Open Circuit Voltage; KF = Kalman Filter.

Table II shows more detailed results about quantitative data errors. Practically, SOC estimation results frequently depend on its initialization; the initialization process becomes significant when the method cannot correct the initialization error. In this research, two methods could not correct the SOC initialization error: Coulomb Counting and OCV methods based on Model 2. Meanwhile, the OCV Model 3 method, Kalman Filter Model 1, and Kalman Filter Model 2 could perform the correction.

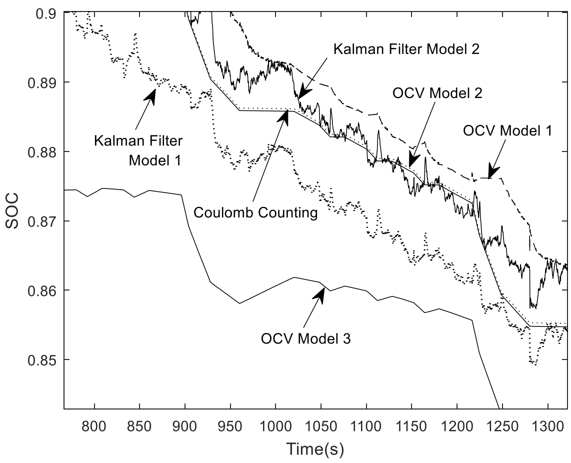

Fig. 4. SOC Estimation with Pulse Test Data

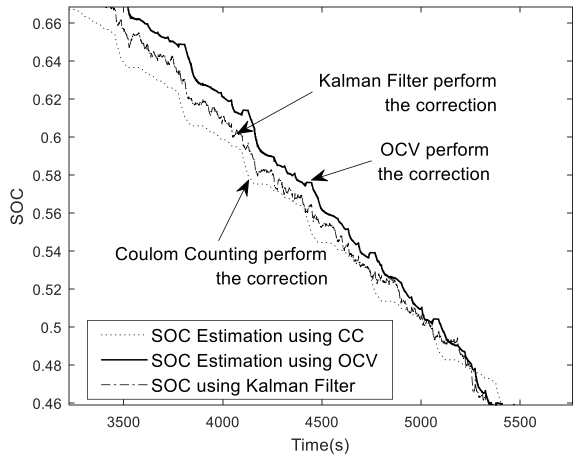

Fig. 5. Comparison of Correction Capability in SOC Estimation Methods

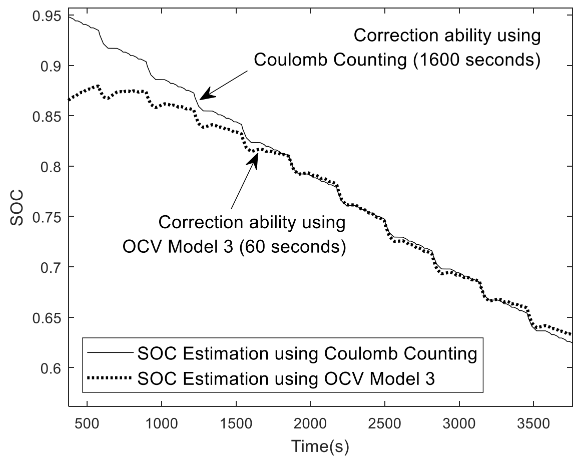

Fig. 6. SOC Initialization of Coulomb Counting and OCV Model 3

Meanwhile, Figure 6 shows the estimation results using Coulomb Counting and OCV Model 3. Even though the initialization error was too far from its actual value, the two methods could perform estimation correction. The Coulomb Counting method took 1600 seconds, while the OCV Model 3 only took 60 seconds to correct the SOC value.

B. SOC Estimation Results with Dynamic Stress Test (DST) Data

Tests were also carried out with varying loads. Figure 7 shows a comparison of the SOC estimation methods used in the Coulomb Counting and OCV Model. Tests were carried out until the battery had a capacity of 20%. Table III shows the error data for each SOC estimation method.

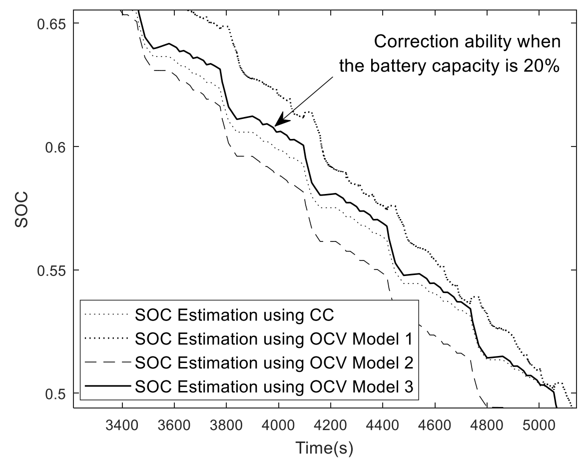

Fig. 7. Comparison of Variable Load SOC Estimation Methods

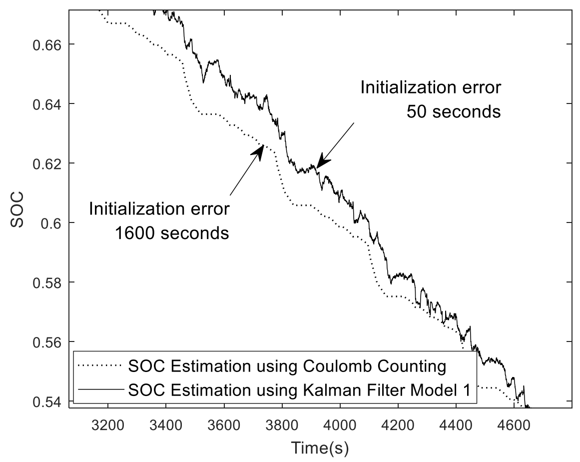

Fig. 8. Comparison of The Correction Ability of The SOC Estimation Method

Table 3 presents the Mean Square Error (MSE), which is a parameter that shows the average square between the actual data and the estimated data. In comparison, the Root Mean Square Error (RMSE) is an indicator of error which is translated as the square root of the average difference between the real data and the estimated data. This parameter indicates a fairly high significant effect in the estimation results. The accuracy of modelling can be measured relatively using the MSE parameter.

The OCV estimation results were obtained from model 3 with the recursive equation obtained from the pulse test data. From the OCV value, it is entered into the equation function of the relationship between OCV-SOC to get the SOC value.

The initialization error of the SOC value was tested to compare the reliability of the SOC estimation methods. Figure 8 shows the ability of the two methods to correct SOC initialization error; the initialized SOC was 80% when the actual value was 100%. The Kalman Filter Model 1 only required 50 seconds, while the Coulomb Counting method took 1600 seconds.

TABLE III
ERROR SOC ESTIMATION WITH DST DATA

Method	Final SOC	% ERROR	MSE	RMSE
CC	21.68%	11.136	24×10^{-5}	0.0186
OCV 1	19.77 %	1.9184	17.55×10^{-5}	0.0132
OCV 2	17.38 %	3.44	27.3×10^{-5}	0.0165
OCV 3	18.20 %	1.86	7.725×10^{-5}	0.0088
KF 1	20.04 %	0.2612	0.19×10^{-5}	0.0014
KF 2	19.42 %	0.6661	12.44×10^{-5}	0.0031

[a]CC = Coulomb Counting, OCV = Open Circuit Voltage; KF = Kalman Filter.

The smallest error value/MSE was obtained from the implementation of the Kalman Filter. The varying load used was 0.0011 with a final SOC value of 20.04%; MSE was 0.19 x 10-5 with an error percentage of 0.261; and RMSE of 0.0014.

Meanwhile, the largest error value was shown by the OCV algorithm with an MSE of 17.38%; a final SOC value of 0.0124; MSE is 27.3 x 10-5 with an error percentage of 3.44; and RMSE of 0.0165.

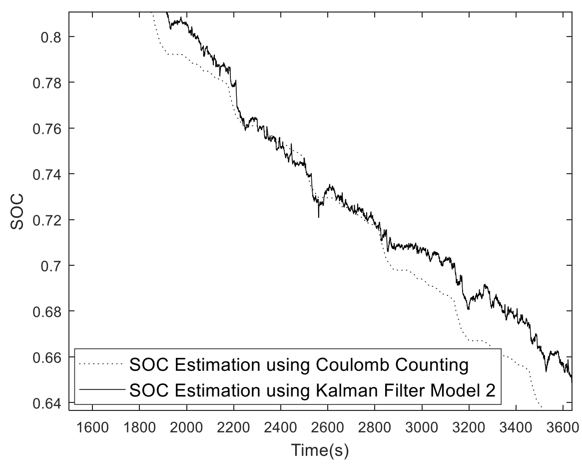

Fig. 9. Comparison of The Correction Ability of The SOC Estimation Method (3600 seconds)

Initialization error is done by initializing SOC with 0%. Figure 9 shows that both methods can correct the SOC value but need to be clarified in Figure 10.

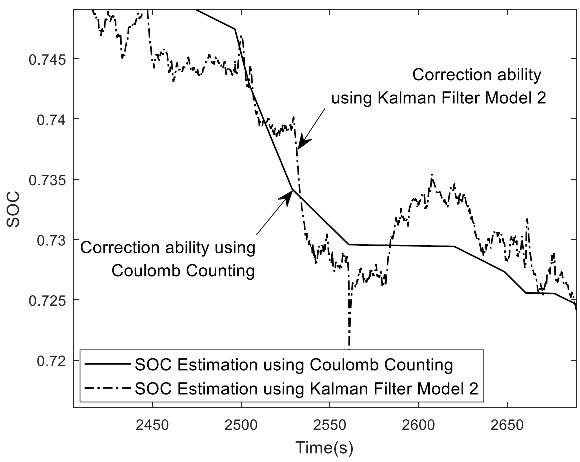

Fig. 10. Comparison of The Correction Ability of The SOC Estimation Method (2650 seconds)

An extreme initialization error test was also performed by initializing the SOC with 0%. Figure 10 shows that the two methods could correct the SOC value. However, the Coulomb Counting method needed a longer time (1600 seconds) than the Kalman Filter Model 2, which only took 50 seconds.

V. Conclusion

This research has conducted simulations of SOC estimation using a combinations of battery model and estimation method. The SOC estimation using the Coulomb Counting method was highly dependent upon the accuracy of the current sensor. Then, the SOC estimation based on battery modelling could result in an accurate estimation. However, only the Kalman Filter algorithm could produce an accurate SOC estimation and quickly correct the initialization error of the SOC value with the smallest error value: MAE 0.001; MSE 0.19 x 10-5; and RMSE 0.0014. Therefore, this research conclude that the SOC estimation method of battery in the BMS of an electric vehicle should be done by using Kalman Filter algorithm.

References

[1] X. Kuang *et al.*, “Research on Control Strategy for a Battery Thermal Management System for Electric Vehicles Based on Secondary Loop Cooling,” *IEEE Access*, vol. 8, pp. 73475–73493, 2020, doi: 10.1109/ACCESS.2020.2986814.

[2] J. Yang, W. Wang, K. Ma, and B. Yang, “Optimal Dispatching Strategy for Shared Battery Station of Electric Vehicle by Divisional Battery Control,” *IEEE Access*, vol. 7, pp. 38224–38235, 2019, doi: 10.1109/ACCESS.2019.2906488.

[3] H. Kikusato *et al.*, “Electric Vehicle Charge-Discharge Management for Utilization of Photovoltaic by Coordination between Home and Grid Energy Management Systems,” *IEEE Trans. Smart Grid*, vol. 10, no. 3, pp. 3186–3197, 2019, doi: 10.1109/TSG.2018.2820026.

[4] A. Fathy, M. Al-Dhaifallah, and H. Rezk, “Recent Coyote Algorithm-Based Energy Management Strategy for Enhancing Fuel Economy of Hybrid FC/Battery/SC System,” *IEEE Access*, vol. 7, pp. 179409–179419, 2019, doi: 10.1109/ACCESS.2019.2959547.

[5] J. Hong, J. Yin, Y. Liu, J. Peng, and H. Jiang, “Energy Management and Control Strategy of Photovoltaic/Battery Hybrid Distributed Power Generation Systems with an Integrated Three-Port Power Converter,” *IEEE Access*, vol. 7, pp. 82838–82847, 2019, doi: 10.1109/ACCESS.2019.2923458.

[6] R. Hemmati and H. Mehrjerdi, “Stochastic linear programming for optimal planning of battery storage systems under unbalanced-uncertain conditions,” *J. Mod. Power Syst. Clean Energy*, vol. 8, no. 5, pp. 971–980, 2020, doi: 10.35833/MPCE.2019.000324.

[7] X. Liu *et al.*, “Online identification of power battery parameters for electric vehicles using a decoupling multiple forgetting factors recursive least squares method,” *CSEE J. Power Energy Syst.*, vol. 6, no. 3, pp. 735–742, 2020, doi: 10.17775/CSEEJPES.2018.00960.

[8] M. Kim, K. Kim, and S. Han, “Reliable Online Parameter Identification of Li-Ion Batteries in Battery Management Systems Using the Condition Number of the Error Covariance Matrix,” *IEEE Access*, vol. 8, pp. 189106–189114, 2020, doi: 10.1109/access.2020.3031500.

[9] M. Hossain, S. Saha, M. T. Arif, A. M. T. Oo, N. Mendis, and M. E. Haque, “A Parameter Extraction Method for the Li-Ion Batteries with Wide-Range Temperature Compensation,” *IEEE Trans. Ind. Appl.*, vol. 56, no. 5, pp. 5625–5636, 2020, doi: 10.1109/TIA.2020.3011385.

[10] S. Liu, J. Wang, Q. Liu, J. Tang, H. Liu, and Z. Fang, “Deep-Discharging Li-Ion Battery State of Charge Estimation Using a Partial Adaptive Forgetting Factors Least Square Method,” *IEEE Access*, vol. 7, pp. 47339–47352, 2019, doi: 10.1109/ACCESS.2019.2909274.

[11] A. Ito, A. Kawashima, T. Suzuki, S. Inagaki, T. Yamaguchi, and Z. Zhou, “Model Predictive Charging Control of In-Vehicle Batteries for Home Energy Management Based on Vehicle State Prediction,” *IEEE Trans. Control Syst. Technol.*, vol. 26, no. 1, pp. 51–64, 2018, doi: 10.1109/TCST.2017.2664727.

[12] A. Q. Tameemi, “Fusion-based deterministic and stochastic parameters estimation for a lithium-polymer battery model,” *IEEE Access*, vol. 8, pp. 193005–193019, 2020, doi: 10.1109/ACCESS.2020.3033497.

[13] N. Chen, P. Zhang, J. Dai, and W. Gui, “Estimating the State-of-Charge of Lithium-Ion Battery Using an H-Infinity Observer Based on Electrochemical Impedance Model,” *IEEE Access*, vol. 8, pp. 26872–26884, 2020, doi: 10.1109/ACCESS.2020.2971002.

[14] S. Afshar, K. Morris, and A. Khajepour, “State-of-Charge Estimation Using an EKF-Based Adaptive Observer,” *IEEE Trans. Control Syst. Technol.*, vol. PP, pp. 1–17, 2018, doi: 10.1109/TCST.2018.2842038.

[15] M. Seo, M. Park, Y. Song, and S. W. Kim, “Online Detection of Soft Internal Short Circuit in Lithium-Ion Batteries at Various Standard Charging Ranges,” *IEEE Access*, vol. 8, pp. 70947–70959, 2020, doi: 10.1109/ACCESS.2020.2987363.

[16] S. Lee, P. Mohtat, J. B. Siegel, A. G. Stefanopoulou, J. W. Lee, and T. K. Lee, “Estimation Error Bound of Battery Electrode Parameters with Limited Data Window,” *IEEE Trans. Ind. Informatics*, vol. 16, no. 5, pp. 3376–3386, 2020, doi: 10.1109/TII.2019.2952066.

[17] K. Sarrafan, K. M. Muttaqi, and D. Sutanto, “Real-Time Estimation of Model Parameters and State-of-Charge of Li-Ion Batteries in Electric Vehicles Using a New Mixed Estimation Model,” *IEEE Trans. Ind. Appl.*, vol. 56, no. 5, pp. 5417–5428, 2020, doi: 10.1109/TIA.2020.3002977.

[18] A. Fotouhi, D. J. Auger, K. Propp, and S. Longo, “Accuracy Versus Simplicity in Online Battery Model Identification,” *IEEE Trans. Syst. Man, Cybern. Syst.*, vol. 48, no. 2, pp. 195–206, 2018, doi: 10.1109/TSMC.2016.2599281.

[19] X. Zan, Z. Jiang, K. Ni, W. Zhang, Y. Gong, and N. Wu, “Modular battery management for SRM drives in hybrid vehicles based on a novel modular converter,” *IEEE Access*, vol. 8, pp. 136296–136306, 2020, doi: 10.1109/ACCESS.2020.3011451.

[20] L. Xuan, L. Qian, J. Chen, X. Bai, and B. Wu, “State-of-charge prediction of battery management system based on principal component analysis and improved support vector machine for regression,” *IEEE Access*, vol. 8, pp. 164693–164704, 2020, doi: 10.1109/ACCESS.2020.3021745.

[21] H. Aung, J. J. Soon, S. T. Goh, J. M. Lew, and K. S. Low, “Battery Management System with State-of-Charge and Opportunistic State-of-Health for a Miniaturized Satellite,” *IEEE Trans. Aerosp. Electron. Syst.*, vol. 56, no. 4, pp. 2978–2989, 2020, doi: 10.1109/TAES.2019.2958161.

[22] Z. Huang, F. Yang, F. Xu, X. Song, and K. L. Tsui, “Convolutional Gated Recurrent Unit-Recurrent Neural Network for State-of-Charge Estimation of Lithium-Ion Batteries,” *IEEE Access*, vol. 7, pp. 93139–93149, 2019, doi: 10.1109/ACCESS.2019.2928037.

[23] X. Song, F. Yang, D. Wang, and K. L. Tsui, “Combined CNN-LSTM Network for State-of-Charge Estimation of Lithium-Ion Batteries,” *IEEE Access*, vol. 7, pp. 88894–88902, 2019, doi:

10.1109/ACCESS.2019.2926517.
[24] X. Wu, X. Li, and J. Du, "State of Charge Estimation of Lithium-Ion Batteries over Wide Temperature Range Using Unscented Kalman Filter," *IEEE Access*, vol. 6, pp. 41993–42003, 2018, doi: 10.1109/ACCESS.2018.2860050.
[25] D. Xiao *et al.*, "Reduced-Coupling Coestimation of SOC and SOH for Lithium-Ion Batteries Based on Convex Optimization," *IEEE Trans. Power Electron.*, vol. 35, no. 11, pp. 12332–12346, 2020, doi: 10.1109/TPEL.2020.2984248.
[26] K. Sarrafan, K. M. Muttaqi, and D. Sutanto, "Real-time state-of-charge tracking system using mixed estimation algorithm for electric vehicle battery system," *2018 IEEE Ind. Appl. Soc. Annu. Meet. IAS 2018*, pp. 1–8, 2018, doi: 10.1109/IAS.2018.8544613.
[27] G. Dong, Z. Chen, and J. Wei, "Sequential Monte Carlo Filter for State-of-Charge Estimation of Lithium-Ion Batteries Based on Auto Regressive Exogenous Model," *IEEE Trans. Ind. Electron.*, vol. 66, no. 11, pp. 8533–8544, 2019, doi: 10.1109/TIE.2018.2890499.
[28] R. Xiong, J. Cao, Q. Yu, H. He, and F. Sun, "Critical Review on the Battery State of Charge Estimation Methods for Electric Vehicles," *IEEE Access*, vol. 6, pp. 1832–1843, 2017, doi: 10.1109/ACCESS.2017.2780258.
[29] K. Mahmud, M. J. Hossain, and G. E. Town, "Peak-Load Reduction by Coordinated Response of Photovoltaics, Battery Storage, and Electric Vehicles," *IEEE Access*, vol. 6, pp. 29353–29365, 2018, doi: 10.1109/ACCESS.2018.2837144.
[30] W. Wang, X. Wang, C. Xiang, C. Wei, and Y. Zhao, "Unscented kalman filter-based battery SOC estimation and peak power prediction method for power distribution of hybrid electric vehicles," *IEEE Access*, vol. 6, pp. 35957–35965, 2018, doi: 10.1109/ACCESS.2018.2850743.
[31] Z. Xi, M. Dahmardeh, B. Xia, Y. Fu, and C. Mi, "Learning of Battery Model Bias for Effective State of Charge Estimation of Lithium-Ion Batteries," *IEEE Trans. Veh. Technol.*, vol. 68, no. 9, pp. 8613–8628, 2019, doi: 10.1109/TVT.2019.2929197.
[32] M. Park, M. Seo, Y. Song, and S. W. Kim, "Capacity Estimation of Li-Ion Batteries Using Constant Current Charging Voltage with Multilayer Perceptron," *IEEE Access*, vol. 8, pp. 180762–180772, 2020, doi: 10.1109/ACCESS.2020.3028095.
[33] S. Yang, Y. Cao, S. Zhou, Y. Hua, X. Zhou, and X. Liu, "A Comprehensive Evaluation on Variable Sampling Intervals of Power Battery System for Electric Vehicles," *IEEE Access*, vol. 8, pp. 156232–156243, 2020, doi: 10.1109/ACCESS.2020.3011880.
[34] D. Liu, X. Yin, Y. Song, W. Liu, and Y. Peng, "An on-line state of health estimation of lithium-ion battery using unscented particle filter," *IEEE Access*, vol. 6, pp. 40990–41001, 2018, doi: 10.1109/ACCESS.2018.2854224.
[35] D. N. T. How, M. A. Hannan, M. S. Hossain Lipu, and P. J. Ker, "State of Charge Estimation for Lithium-Ion Batteries Using Model-Based and Data-Driven Methods: A Review," *IEEE Access*, vol. 7, pp. 136116–136136, 2019, doi: 10.1109/ACCESS.2019.2942213.
[36] R. Hasan and J. Scott, "Extending Randles's Battery Model to Predict Impedance, Charge-Voltage, and Runtime Characteristics," *IEEE Access*, vol. 8, pp. 85321–85328, 2020, doi: 10.1109/ACCESS.2020.2992771.
[37] H. Karlsen, T. Dong, Z. Yang, and R. Carvalho, "Temperature-dependence in battery management systems for electric vehicles: Challenges, criteria, and solutions," *IEEE Access*, vol. 7, pp. 142203–142213, 2019, doi: 10.1109/ACCESS.2019.2943558.

Lora Khaula Amifia, S.Pd., M.Eng. was born on June 06, 1992, in Mojokerto (East Java, Indonesia). This author became a Member (M) of IAENG in 2021. She is a Lecturer in the Faculty of Electrical Engineering and Intelligent Industry, Institut Teknologi Telkom Surabaya, Indonesia. She received an S.Pd degree from the State University of Malang, Malang, Indonesia in 2014. She did M.Eng. degree at in Universitas Gadjah Mada, Yogyakarta, Indonesia in 2016 and her research interests are Control Engineering, Non Linear System, Artificial Intellegent.